isvr Institute of Sound and Vibration Research

Time Domain Source Signal Reconstruction Using Beamforming Techniques

J. Rose and P.A. Nelson

ISVR Technical Memorandum No 948

June 2005

University of Southampton

SCIENTIFIC PUBLICATIONS BY THE ISVR

Technical Reports are published to promote timely dissemination of research results by ISVR personnel. This medium permits more detailed presentation than is usually acceptable for scientific journals. Responsibility for both the content and any opinions expressed rests entirely with the author(s).

Technical Memoranda are produced to enable the early or preliminary release of information by ISVR personnel where such release is deemed to the appropriate. Information contained in these memoranda may be incomplete, or form part of a continuing programme; this should be borne in mind when using or quoting from these documents.

Contract Reports are produced to record the results of scientific work carried out for sponsors, under contract. The ISVR treats these reports as confidential to sponsors and does not make them available for general circulation. Individual sponsors may, however, authorize subsequent release of the material.

UNIVERSITY OF SOUTHAMPTON

INSTITUTE OF SOUND AND VIBRATION RESEARCH

FLUID DYNAMICS AND ACOUSTICS GROUP

Time Domain Source Signal Reconstruction Using Beamforming Techniques

by

J Rose and P A Nelson

ISVR Technical Memorandum No. 948

June 2005

Authorized for issue by
Professor V F Humphrey

CONTENTS

LIST OF TABLES

LIST OF FIGURES

ABSTRACT

The performance of several different beamforming techniques in their ability to estimate the time domain signal of a monopole source is considered under varying conditions of signal-to-noise-ratio and the number of uncorrelated sound sources present. The geometric layout is that of a 33^{rd} scale model of an engine test cell with a 62-microphone spiral array. The best performance was achieved with a method that takes advantage of a reference signal of the target sound source being present as long as the reference signal is not significantly influenced by other sources. One of the methods that utilise the eigenvalue-eigenvector decomposition of the cross-spectral matrix of the received array signals was found to perform least well. Several other methods' performance were quite similar at a performance level in-between these other two.

I. INTRODUCTION

Beamforming methods generally utilise signal processing on data received by an array of receivers to locate and estimate the strength of a distribution of sources in space. This memorandum presents some computer simulations undertaken in order to consider how well several different beamforming techniques perform at finding the time-domain source signal emitted by sound sources. Note that this goal is slightly different than the usual intended goal of beamforming to locate sources and estimate source strength. Section 2 describes the problem of a single source in free space and the presents the beamforming methods that are undertaken in the simulations that follow. Section 3 describes the multi-source problem and the two different beamforming methods attempted in the multi-source simulations. The simulation results are presented and discussed in section 4.

The following description of the problem is restricted to the discrete frequency domain where k is the integer frequency sample index. A more detailed review of the methods discussed below is given by Nelson [1].

II. SINGLE-SOURCE METHODS

A single monopole sound source of strength or volume acceleration $V(k)$ emits sound into free space to an array of M receivers. The transfer functions from the sound source to M receivers are defined by the Green function vector

$$\mathbf{g}^{\mathrm{T}} = \begin{bmatrix} G_1(k) & G_2(k) & \cdots & G_M(k) \end{bmatrix} \tag{1}$$

where $G_i(k)$ is a Green function describing the response of the acoustic path from the acoustic source to receiver i and the superscript T is the transpose operator. The signals picked up by the receivers

$$\mathbf{x}^{\mathrm{T}} = \begin{bmatrix} X_1(k) & X_2(k) & \cdots & X_M(k) \end{bmatrix} \tag{2}$$

are the combination of the signals due to the sound source

$$\mathbf{s}^{\mathrm{T}} = V(k)\mathbf{g}^{\mathrm{T}} = \begin{bmatrix} S_1(k) & S_2(k) & \cdots & S_M(k) \end{bmatrix} \tag{3}$$

and noise

$$\mathbf{n}^{\mathrm{T}} = \begin{bmatrix} N_1(k) & N_2(k) & \cdots & N_M(k) \end{bmatrix} \tag{4}$$

so that

$$\mathbf{x} = V(k)\mathbf{g} + \mathbf{n} = \mathbf{s} + \mathbf{n} \tag{5}$$

The receiver signals $\mathbf{x}$ are filtered by a filter vector

$$\mathbf{w}^{\mathrm{H}} = [W_1^*(k) \quad W_2^*(k) \quad \cdots \quad W_M^*(k)] \tag{6}$$

to produce the beamformer output

$$Y(k) = \mathbf{w}^{\mathrm{H}}\mathbf{x} \tag{7}$$

where * denotes complex conjugate and the superscript H denotes the complex conjugate transpose. The goal is to design the filter vector $\mathbf{w}^{\mathrm{H}}$ so that the output of the beamformer $Y(k)$ approximates the source output $V(k)$. The error

$$E(k) = Y(k) - V(k) \tag{8}$$

helps to evaluate the performance of the filter design. A symmetric matrix of cross spectra of the receiver data $\mathbf{x}$, utilised in several of the beamforming methods, is defined by

$$\mathbf{S}_{xx} = E[\mathbf{x}\mathbf{x}^{\mathrm{H}}] \tag{9}$$

where $E[\cdot]$ is the expected value operator.

A. Least squares estimate

The first beamforming method considered finds the filter vector to be the pseudo-inverse of the Green function vector $\mathbf{g}$ [2] i.e.,

$$\mathbf{w}^{\mathrm{H}} = \left(\mathbf{g}^{\mathrm{H}}\mathbf{g}\right)^{-1}\mathbf{g}^{\mathrm{H}}. \tag{10}$$

This is the least squares solution that should minimise the squared error $|E(k)|^2$ of equation (8). Regularisation is sometimes included to help alleviate inversion difficulties. This is done by modifying equation (10) to include a regularisation parameter β of constant real value such that

$$\mathbf{w}^{\mathrm{H}} = \left[\mathbf{g}^{\mathrm{H}}\mathbf{g} + \beta\right]^{-1}\mathbf{g}^{\mathrm{H}}. \tag{11}$$

This method requires knowledge of the Green functions $\mathbf{g}$ but is independent of the receiver data $\mathbf{x}$.

Figure 1 shows a block diagram of the way this least squares estimate was implemented in the time domain for all of the simulations presented in section IV. The first bank of filters are the time reversed Green functions that implement the vector $\mathbf{g}^{\mathrm{H}}$ that is outside of the inversion in equation (11). The inversion is designed in the frequency domain but implemented in the time domain through use of an Inverse Discrete Fourier Transform (IDFT). The value of the advance Δ is related to the size of the Discrete Fourier Transform (DFT) N_{DFT} that was used to find the frequency domain vector of Green functions $\mathbf{g}$, i.e.

$$\Delta = \begin{cases} \frac{3}{2} N_{\mathrm{DFT}} + 1 & \text{for } N_{\mathrm{DFT}} \text{ even} \\ \frac{3}{2}\left(N_{\mathrm{DFT}} + 1\right) & \text{for } N_{\mathrm{DFT}} \text{ odd} \end{cases} \tag{12}$$

For the simulations in the next section the size of the DFT N_{DFT} was equal to the number of samples in the Green functions L.

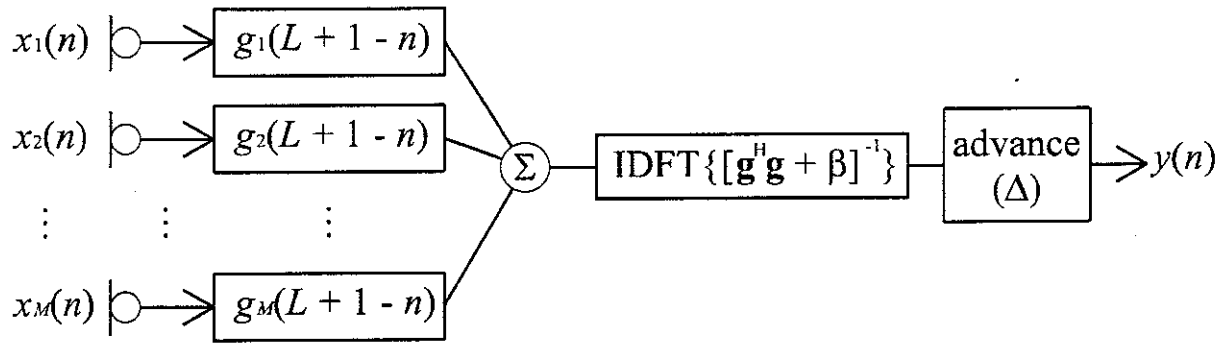

Figure 1 - Block diagram showing the implementation of the 1-source least squares estimation method.

B. Reference signal method

Reference signal beamforming does not require knowledge of the Green functions but does require knowledge of a reference signal that closely represents the source signal $V(k)$ [3]. Besides the cross spectral matrix of equation (9), the column vector of the cross spectra between the receiver data $\mathbf{x}$ and the source signal $V(k)$ is required for this method and is given by

$$\mathbf{s}_{xv} = E[\mathbf{x}V^*(k)] \tag{13}$$

The filter vector is computed as

$$\mathbf{w}^* = \mathbf{S}_{xx}^{-1}\mathbf{s}_{xv}. \tag{14}$$

Regularisation can be utilised to aid the possibly problematic matrix inversion due to singularity or near-singularity of the matrix so that equation (14) becomes

$$\mathbf{w}^* = \left[\mathbf{S}_{xx} + \beta\mathbf{I}\right]^{-1}\mathbf{s}_{xv} \tag{15}$$

where β is the constant real-valued regularisation parameter and $\mathbf{I}$ is the identity matrix. An advantage of this approach is that the direction of the desired signal or the Green functions $\mathbf{g}$ can be unknown.

Figure 2 shows a block diagram of the way this method was implemented in the time domain for all of the simulations presented in section IV. The value of the advance Δ is half of the

DFT size N_{DFT} that was used to find the cross spectral matrix of equation (9) and the cross spectra vector of equation (13). For the simulations in section IV, $N_{DFT} = 1024$ and $\Delta = 512$.

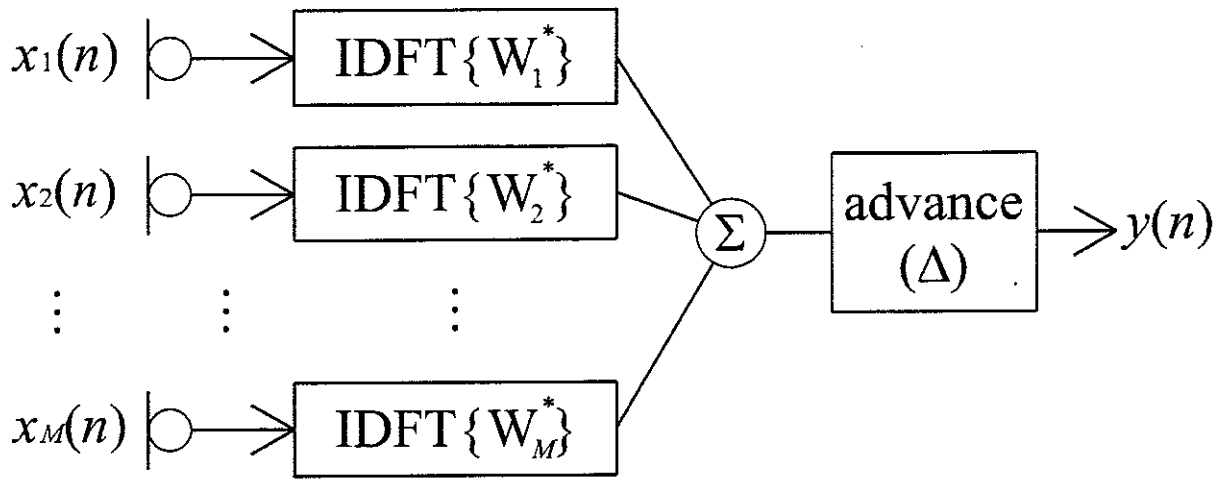

Figure 2 - Block diagram showing the way the 1-source reference signal method, minimum variance method, eigenvector method, and MUSIC method were implemented in the time domain for the simulations in section IV.

C. Minimum variance method

Minimum variance beamforming is a popular approach that is based on Capon's method [4]. The variance of the array output is minimised while a unity gain is preserved for the "look" direction defined by the Green functions. The filter vector for this method is [5]

$$\mathbf{w} = \frac{\mathbf{S}_{xx}^{-1}\mathbf{g}}{\mathbf{g}^{H}\mathbf{S}_{xx}^{-1}\mathbf{g}} \tag{16}$$

Regularisation can be applied to the inversion so that

$$\mathbf{w} = \frac{\left[\mathbf{S}_{xx} + \beta\mathbf{I}\right]^{-1}\mathbf{g}}{\mathbf{g}^{H}\left[\mathbf{S}_{xx} + \beta\mathbf{I}\right]^{-1}\mathbf{g}}. \tag{17}$$

Figure 2 shows a block diagram of the way this method was implemented in the time domain for all of the simulations presented in section IV. The value of the advance Δ is half of the DFT size N_{DFT} that was used to find the cross spectral matrix of equation (9) and also the frequency domain vector of Green functions $\mathbf{g}$. For the simulations in section IV, $N_{DFT} = 1024$ and $\Delta = 512$.

D. Eigenvector method

The eigenvector method [6] is similar to the minimum variance method above but is based on an eigenvector-eigenvalue decomposition of the cross spectral matrix of the receiver data $\mathbf{S}_{xx}$. The eigenvectors of $\mathbf{S}_{xx}$ are $\mathbf{u}_1$, $\mathbf{u}_2$, $\cdots$ $\mathbf{u}_M$, which correspond to eigenvalues

$\lambda_1, \ \lambda_2, \ \cdots \ \lambda_M$ where $\lambda_1 \geq \lambda_2 \geq \cdots \geq \lambda_M$. Any eigenvector $\mathbf{u}_i$ is made up of M elements so that

$$\mathbf{u}_i^{\mathrm{T}} = [U_{1i}(k) \ \ U_{2i}(k) \ \ \cdots \ \ U_{Mi}(k)]. \tag{18}$$

The filter vector is found by

$$\mathbf{w} = \frac{\mathbf{S}_{ev}^{-1}\mathbf{g}}{\mathbf{g}^{\mathrm{H}}\mathbf{S}_{ev}^{-1}\mathbf{g}} \tag{19}$$

where

$$\mathbf{S}_{ev}^{-1} = \sum_{i=S+1}^{M} \frac{1}{\lambda_i}\mathbf{u}_i\mathbf{u}_i^{\mathrm{H}} \tag{20}$$

and S is the number of incoherent linearly independent sources present (equal to one in the present single-source case).

Figure 2 shows a block diagram of the way this method was implemented in the time domain for all of the simulations presented in section IV. The value of the advance Δ is half of the DFT size N_{DFT} that was used to find the cross spectral matrix of equation (9). For the simulations in section IV, $N_{\mathrm{DFT}} = 1024$ and $\Delta = 512$.

E. MUSIC method

The multiple signal classification (MUSIC) algorithm [7] is a slightly modified version of the eigenvector method described above. The filter vector is

$$\mathbf{w} = \frac{\mathbf{S}_M^{-1}\mathbf{g}}{\mathbf{g}^{\mathrm{H}}\mathbf{S}_M^{-1}\mathbf{g}} \tag{21}$$

where

$$\mathbf{S}_M^{-1} = \sum_{i=S+1}^{M} \mathbf{u}_i\mathbf{u}_i^{\mathrm{H}}. \tag{22}$$

Figure 2 shows a block diagram of the way this method was implemented in the time domain for all of the simulations presented in section IV. The value of the advance Δ is half of the DFT size N_{DFT} that was used to find the cross spectral matrix of equation (9). For the simulations in section IV, $N_{\mathrm{DFT}} = 1024$ and $\Delta = 512$.

III. MULTI-SOURCE METHODS

With multiple sources present (i.e. $S > 1$) a source strength vector is defined by

$$\mathbf{v}^{\mathrm{T}} = \begin{bmatrix} V_1(k) & V_2(k) & \cdots & V_S(k) \end{bmatrix}. \tag{23}$$

A $M \times S$ Green function matrix describing the acoustic responses of the paths from S sources to M receivers is

$$\mathbf{G} = \begin{bmatrix} G_{11}(k) & G_{12}(k) & \cdots & G_{1S}(k) \\ G_{21}(k) & G_{22}(k) & \cdots & G_{2S}(k) \\ \vdots & \vdots & \ddots & \vdots \\ G_{M1}(k) & G_{M2}(k) & \cdots & G_{MS}(k) \end{bmatrix} = \begin{bmatrix} \mathbf{g}_1 & \mathbf{g}_2 & \cdots & \mathbf{g}_S \end{bmatrix}. \tag{24}$$

The vector of received signals at the M receivers $\mathbf{x}$ are a combination of the signals due to the sources and noise, i.e.

$$\mathbf{x} = \mathbf{G}\mathbf{v} + \mathbf{n}\,. \tag{25}$$

The receiver signals $\mathbf{x}$ are filtered with a $M \times S$ matrix of filters

$$\mathbf{W} = \begin{bmatrix} W_{11}(k) & W_{12}(k) & \cdots & W_{1S}(k) \\ W_{21}(k) & W_{22}(k) & \cdots & W_{2S}(k) \\ \vdots & \vdots & \ddots & \vdots \\ W_{M1}(k) & W_{M2}(k) & \cdots & W_{MS}(k) \end{bmatrix} = \begin{bmatrix} \mathbf{w}_1 & \mathbf{w}_2 & \cdots & \mathbf{w}_S \end{bmatrix} \tag{26}$$

so that

$$\mathbf{y} = \mathbf{W}^{\mathrm{H}}\mathbf{x} \tag{27}$$

$$\mathbf{y}^{\mathrm{T}} = \begin{bmatrix} Y_1(k) & Y_2(k) & \cdots & Y_S(k) \end{bmatrix} \tag{28}$$

where the beamformer output vector $\mathbf{y}$ is an estimate of the source strength vector $\mathbf{v}$. The vector of error between the beamformer output vector $\mathbf{y}$ and the source strength vector $\mathbf{v}$ is

$$\mathbf{e} = \mathbf{y} - \mathbf{v}\,. \tag{29}$$

A. Multi-source least squares estimate

The matrix of filters for this approach is derived from the pseudo-inverse of the Green function matrix $\mathbf{G}$, i.e. [2]

$$\mathbf{W}^{\mathrm{H}} = \left(\mathbf{G}^{\mathrm{H}}\mathbf{G}\right)^{-1}\mathbf{G}^{\mathrm{H}} \tag{30}$$

Regularisation can be applied to this solution to avoid the effects of ill-conditioning or near singularity in the matrix to be inverted. Equation (30) then becomes

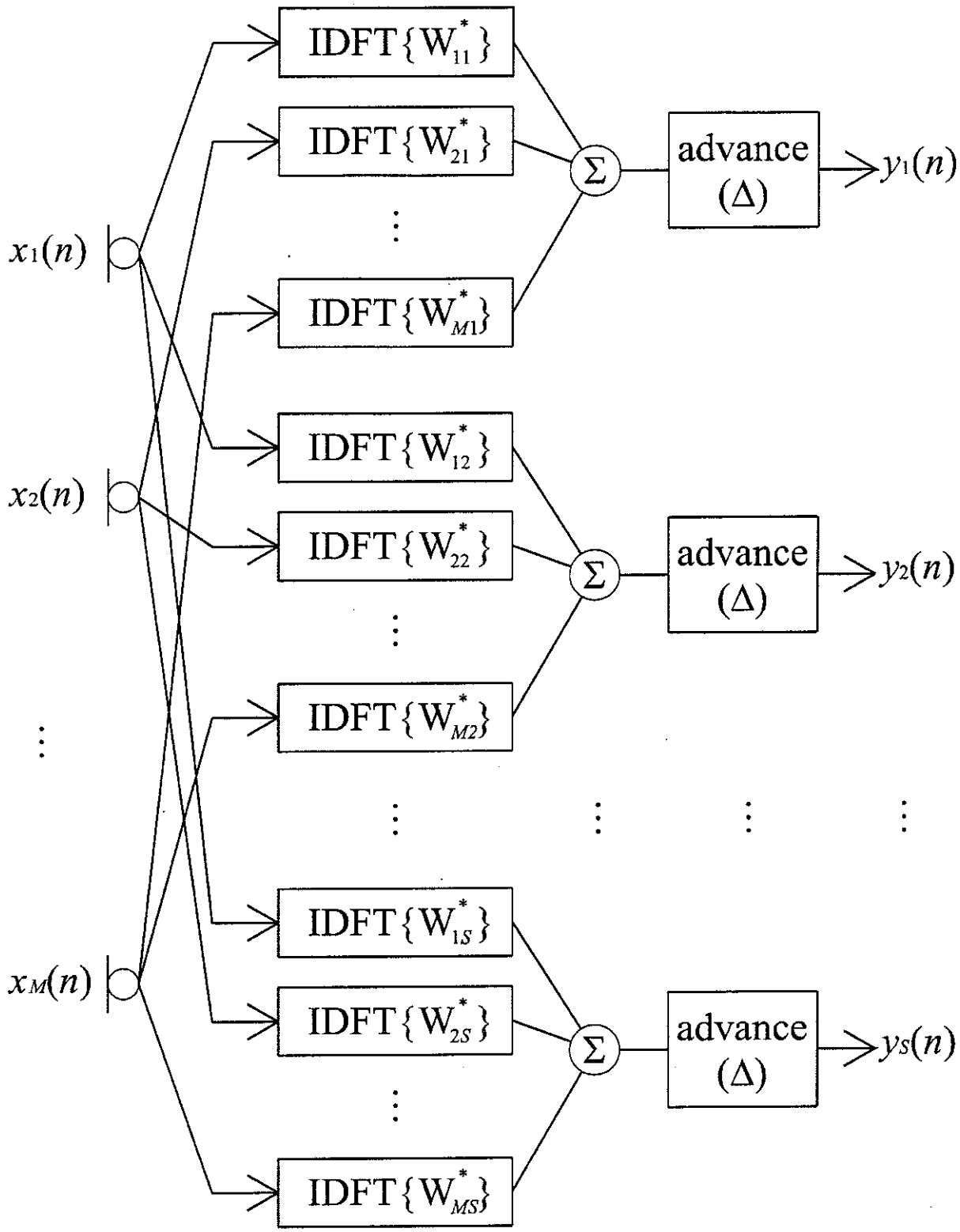

Figure 3 - Block diagram showing the way the multi-source least squares estimation and the multi-source reference signal method were implemented in the time domain for the simulations in section IV.

$$\mathbf{W}^{H} = \left[\mathbf{G}^{H}\mathbf{G} + \beta\mathbf{I}\right]^{-1}\mathbf{G}^{H} \tag{31}$$

Figure 3 shows a block diagram of the way this method was implemented in the time domain for all of the simulations presented in section IV. The value of the advance Δ is half of the DFT size N_{DFT} that was used to find the frequency domain matrix of Green functions **G**. For the simulations in section IV, $N_{\mathrm{DFT}} = 1024$ and $\Delta = 512$.

B. Multi-source reference signal method

A $M \times S$ matrix of cross spectra between receiver signals **x** and source strengths **v** is defined as

$$\mathbf{S}_{xv} = E[\mathbf{x}\mathbf{v}^{\mathrm{H}}]. \tag{32}$$

The matrix of filters is

$$\mathbf{W}^{*} = \mathbf{S}_{xx}^{-1}\mathbf{S}_{xv}. \tag{33}$$

This can be regularised so that equation (33) becomes

$$\mathbf{W}^{*} = \left[\mathbf{S}_{xx} + \beta\mathbf{I}\right]^{-1}\mathbf{S}_{xv}. \tag{34}$$

Figure 3 shows a block diagram of the way this method was implemented in the time domain for all of the simulations presented in section IV. The value of the advance Δ is half of the DFT size N_{DFT} that was used to find the cross spectral matrix of equation (9) and the cross spectral matrix of equation (32). For the simulations in section IV, $N_{\mathrm{DFT}} = 1024$ and $\Delta = 512$.

IV. SIMULATIONS

Performance of the above-described methods in estimating a sound source signal was simulated and results are presented in this section. The sources in the simulations are monopoles emitting white noise into free space. Figure 4 shows a plan view of the geometric layout. The dimensions shown correspond to a 33$^{\mathrm{rd}}$-scale model of an engine test cell. For the simulations here, there is either one source directly in front of the centre of the microphone array or there are multiple uncorrelated sources equally spaced apart that together span a total distance of 0.3m. The target source that is being estimated is always located directly in front of the centre of the array. With 4, 7, 10, 13, and 16 sources, the distance between the sources is 0.1m, 0.05m, 0.033m, 0.025m, and 0.02m respectively. The signals **x** received by the 62 microphone, two-dimensional, spiral array include components due to the source signals **s** as well as added noise **n** (e.g. Equations (5 and 25)). Experimental results of the performance of a larger version of this array were presented by Holland and Nelson [8].

The results of the simulations are considered as a function of signal-to-noise ratio (SNR) defined as

$$\mathrm{SNR} = \frac{\text{array output power due to source}}{\text{array output power due to noise}} \tag{35}$$

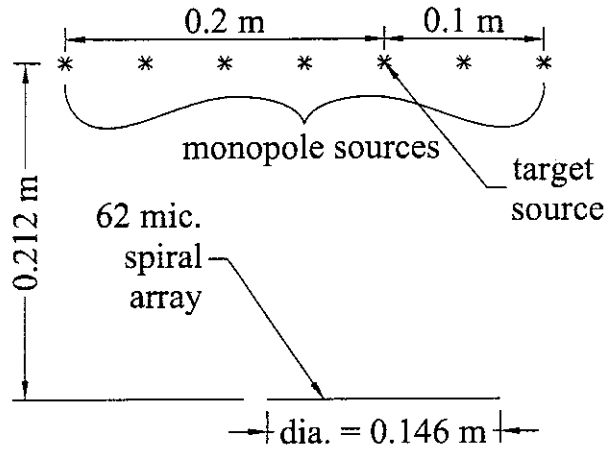

Figure 4 – Plan view of geometrical arrangement for all the simulations.

The measure of performance considered is mean-squared-error (mse) defined as

$$\text{mse} = \frac{1}{Q}\sum_{n=1}^{Q} e^2(n) \tag{36}$$

where Q is the total number of samples available (Q = 4096 throughout these simulations), n is the integer time-domain sampling index, and $e(n)$ is the inverse digital Fourier transform (DFT) of the error $E(k)$ defined in equation (8). The sampling frequency used throughout is 48kHz. Therefore, the results pertain to the full-scale test cell at only frequencies below about 700Hz.

A. Choosing the regularisation parameter

Regularisation was applied to all of the inversions required by the different methods (i.e. equations (11, 15, 17, 31, and 34) were applied). The regularisation parameter β was chosen by looking at the L-curves and selecting the value of β that corresponds to the corner of the curve. The L-curve is a plot on logarithmic scales of the norm of the error versus the norm of the system's solution for varying β [9-10]. Here the sum of squared error $\sum_{n=1}^{Q} e^2(n)$ was plotted versus the sum of the squared output of the beamformer $\sum_{n=1}^{Q} y^2(n)$ to get the L-curves shown in Figures A1-A13 in the appendix. These curves are not shaped in a characteristically L-shape but most do show clear minima in squared error. The regularisation parameters were chosen to minimise the squared error in all of the cases (see Table 1 for the β values chosen). Notice that the chosen value of β varies considerably depending on both the beamforming method and the number of sources.

B. Performance of methods

Figure 5 shows the different methods' mean-squared-error performance with one source present as a function of SNR. With noise present, all of the methods perform similarly well

except for the eigenvector method, which performs poorly. The MUSIC algorithm is the only method that actually performs better with some noise present.

Table 1 – **Chosen values of regularisation parameter.**

METHOD	REGULARISATION PARAMETER β	FIGURE SHOWING L-CURVE
1-Source Least Squares Estimation	0	Figure A 1
1-Source Reference Signal Method	10^{-11}	Figure A 2
Minimum Variance Method	1	Figure A 3
4-Source Least Squares Estimation	8.6×10^{-6}	Figure A 4
7-Source Least Squares Estimation	7×10^{-6}	Figure A 5
10-Source Least Squares Estimation	1.7×10^{-5}	Figure A 6
13-Source Least Squares Estimation	2×10^{-5}	Figure A 7
16-Source Least Squares Estimation	2.5×10^{-5}	Figure A 8
4-Source Reference Signal Method	7×10^{-6}	Figure A 9
7-Source Reference Signal Method	10^{-10}	Figure A 10
10-Source Reference Signal Method	3×10^{-5}	Figure A 11
13-Source Reference Signal Method	0.2	Figure A 12
16-Source Reference Signal Method	0.3	Figure A 13

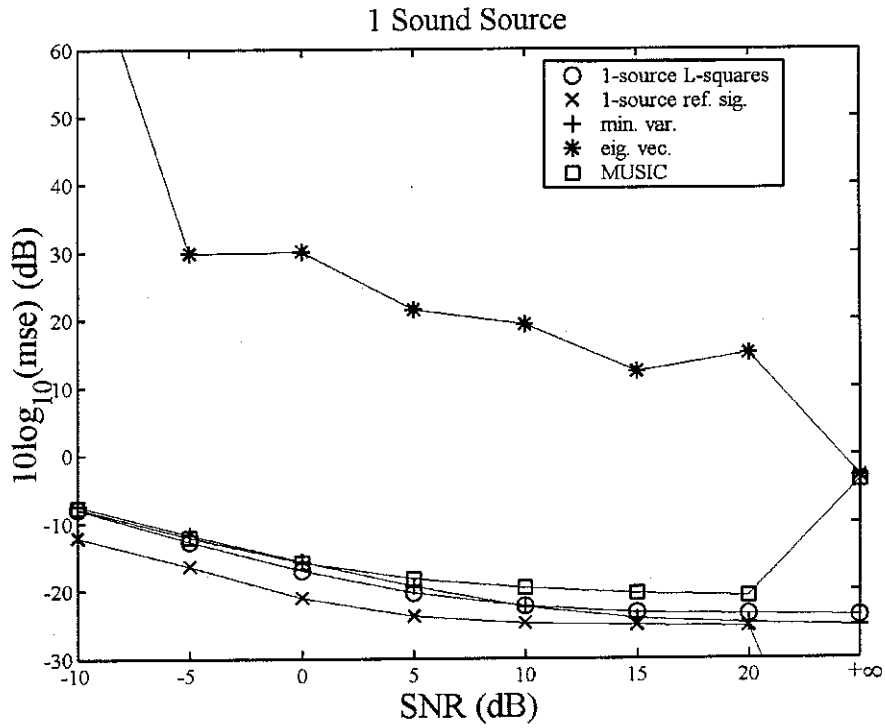

Figure 5 - Mean-squared-error with 1 source present.

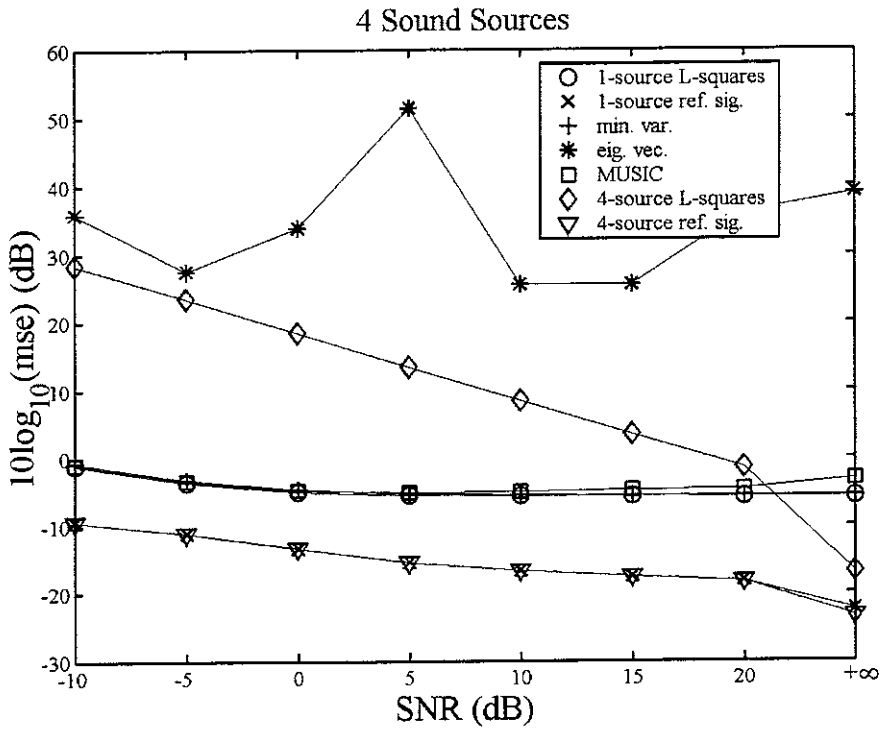

Figure 6 - Mean-squared-error with 4 sources present.

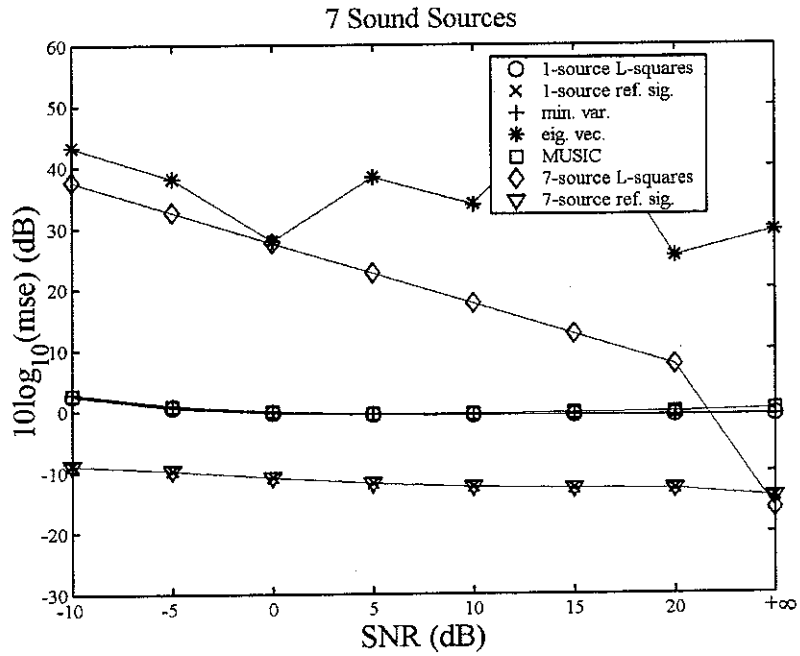

Figure 7 - Mean-squared-error with 7 sources present

Figures 6 and 7 show the results with 4 and 7 sound sources present respectively. The best performance is achieved with either the 1-source or multi-source reference signal methods, which perform similarly. The next best performance with noise present is achieved with the 1-source least squares, minimum variance, and MUSIC methods, which all perform similarly.

The multi-source least squares estimate performs better than these three methods with no noise present but its performance quickly deteriorates with decreasing SNR. The eigenvector method does not appear to perform well at all with multiple sources present.

As a further illustration of the performance of the methods Figure 8 shows 50 samples of the both the target signal and the beamformer output in the digital time domain with 7 sources present and 20dB signal-to-noise-ratio. The methods shown are the 1-source reference signal (a), 1-source least squares (b), 7-source least squares (c), and the eigenvector method (d).

Figure 9 shows the power spectral density of the error for the different methods with 7 sources present and a 0dB SNR as a function of frequency. Here the frequency does not correspond to the 33rd-small scale model of the test cell but the results are scaled up to reflect the results for a full-scale test cell. The sampling frequency of 48kHz used for the small-scale simulation means that the results are only good up to just over 700Hz for the full-scale geometry. The

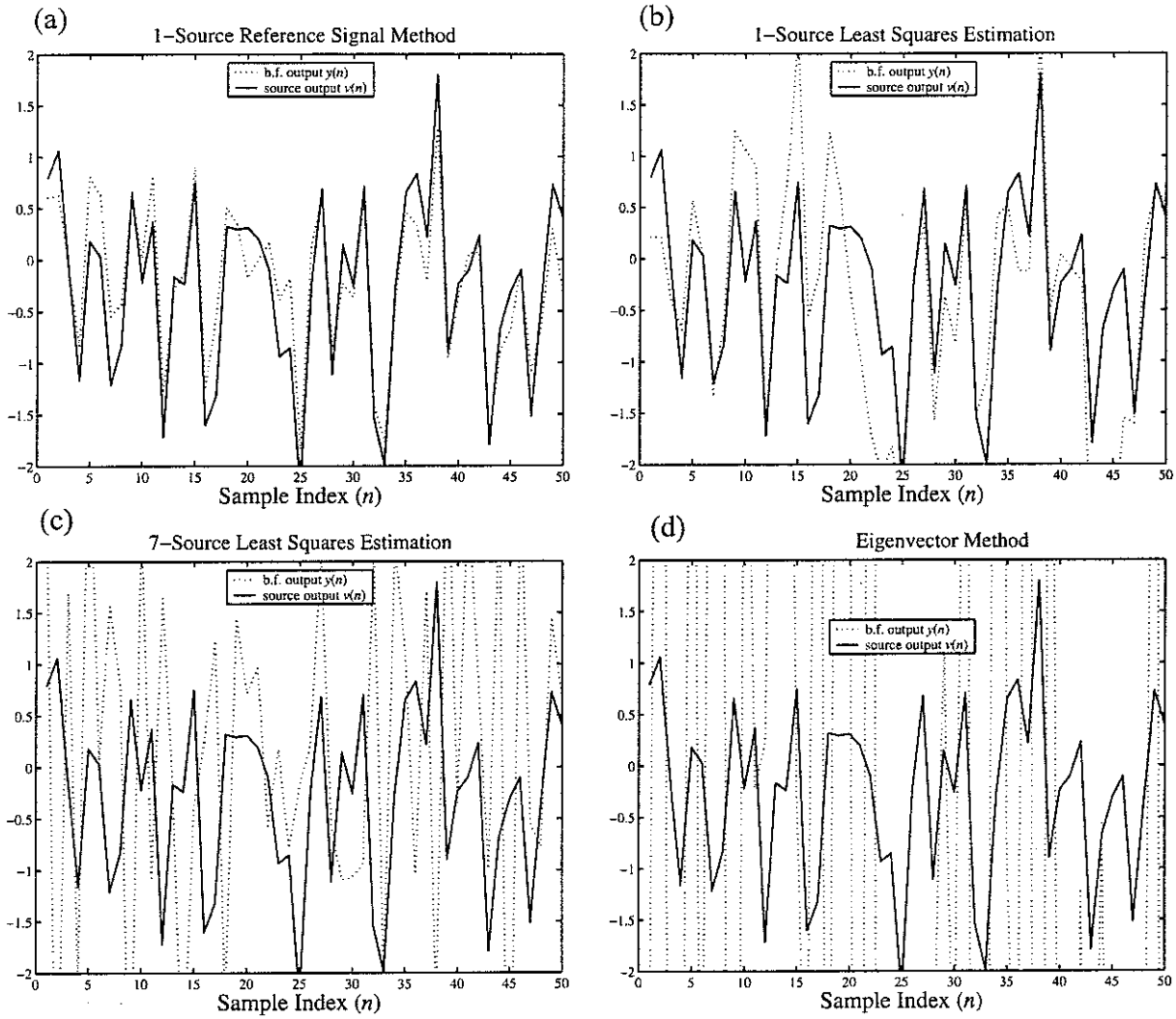

Figure 8 - 50 samples of the time domain source signal $v(n)$ - and output of the beamformer $y(n)$ ... with 7 sources present and SNR = 20dB for (a) 1-source reference signal method, (b) 1-source least squares estimate, (c) 7-source least squares estimation, and the (d) eigenvector method.

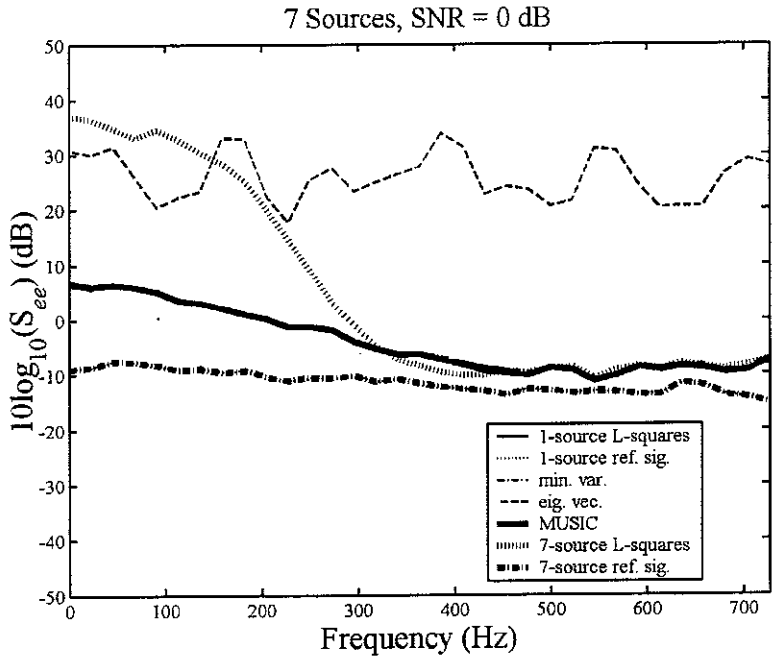

Figure 9 - Power spectral density of the error with 7 sources present and SNR = 0dB for the full-scale test cell.

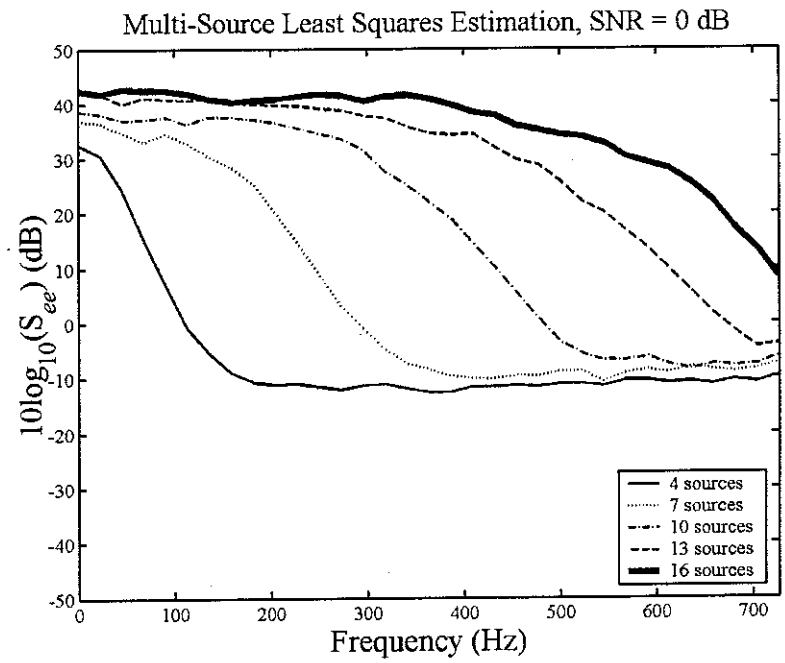

Figure 10 - Power spectral density of the error for multi-source least squares estimation with SNR = 0dB for the full-scale test cell.

performance for the 1-source and the multi-source reference signal methods are indistinguishable as are the 1-source least squares, minimum variance, and MUSIC methods. The multi-source least squares estimation performs similarly to the 1-source least squares method above about 300Hz but much worse below. The performance of the multi-source least squares estimation is shown in Figure 10 as a function of frequency for 4, 7, 10, 13, and 16

sources. The range of frequencies at which good performance is achieved decreases with more sources that are spaced closer together. Perhaps the performance at low frequencies is limited by poor conditioning of the inverse problem that is influenced by the spacing of the sources.

The superiority of the reference signal method is perhaps not surprising given that the method requires knowledge of the signal that it is trying to approximate. In practice, this signal will not be known but an approximation might be known through the use of a reference microphone nearby the sound source that will be receiving not only the target sound source but also any other sound sources nearby. Figure 11 shows the performance of the 1-source reference signal method in estimating the target sound source in the presence of 6 other sound sources as a function of the distance between the reference microphone and the target sound source as the microphone is moved perpendicular to the line of sources toward the microphone array. The performance of the reference signal method decreases to about 0dB at a reference microphone distance of about 0.035m without noise present and about 0.04m with noise. A 0dB mean-squared-error is comparable to the performance of the 1-source least squares, minimum variance, and MUSIC methods with 7 sources. Note that in these simulations when 7 sources are present, the distance between 2 sources is 0.05m.

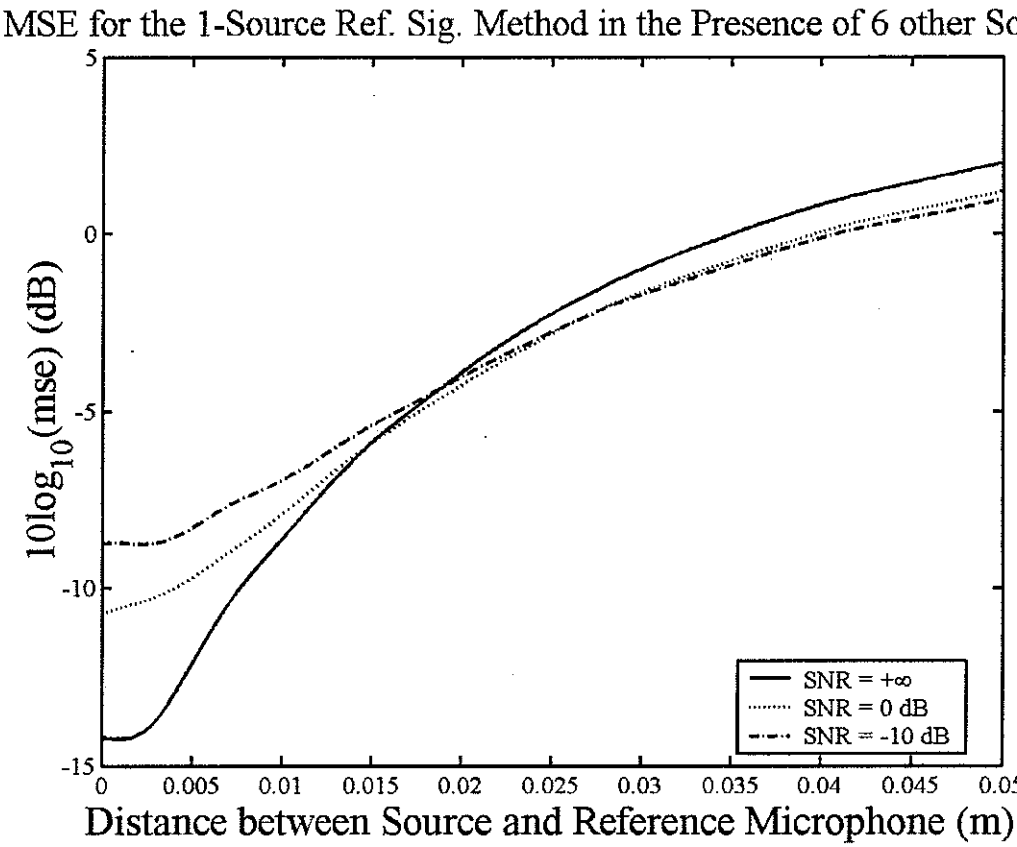

Figure 11 - Mean-squared-error for the 1-source reference signal as a function of distance between the reference microphone and target source in the presence of 6 other sources.

V. CONCLUSION

The simulated beamforming performance was helped by an idealised situation of perfect knowledge of the Green functions, perfectly uncorrelated sound sources, and a perfectly anechoic environment. Keeping this in mind the attempted beamforming techniques were found to be robust to the array's received signals' signal-to-noise-ratio. The best performance was achieved with the reference signal method when the reference microphone was significantly closer to the target sound source than any other sources. The performance of the 1-source least squares estimation, minimum variance, and MUSIC methods were comparable as well as the multi-source least squares estimation above a lower frequency limit that is most likely dictated by the distance between the multiple sources. By far the worst performance was achieved with the eigenvector method.

REFERENCES

[1] P.A. Nelson, "Source identification and location," Chapter 3 in *Advanced Applications in Acoustics, Noise and Vibration* edited by F. Fayh and J. Walker (Spon Press, London and New York, 2004), pp. 100-153

[2] P.A. Nelson and S.H. Yoon, "Estimation of acoustic source strength by inverse methods: Part I, Conditioning of the inverse problem," *Journal of Sound and Vibration* **233**, 643-668 (2000).

[3] B. Widrow, P.E. Mantey, L.J. Griffiths, and B.B. Goode, "Adaptive antenna systems," *Proceedings of the IEEE* **55**, 2143-2159 (1967).

[4] J. Capon, "High-resolution frequency-wavenumber spectrum analysis," *Proceedings of the IEEE* **57**, 1408-1418 (1969).

[5] D.H. Johnson, "The application of spectral estimation methods to bearing estimation problems," *Proceedings of the IEEE* **70**, 1018-1028 (1982).

[6] D.H. Johnson and S.R. DeGraaf, "Improving the resolution of bearing in passive sonar arrays by eigenvalue analysis," *IEEE Transactions on Acoustics, Speech, and Signal Processing* **ASSP-30**, 638-647 (1982).

[7] R.O. Schmidt, "Multiple emitter location and signal parameter estimation," *IEEE Transactions on Antennas and Propagation* **AP-34**, 276-280 (1986).

[8] K.R. Holland and P.A. Nelson, "Sound source characterisation: The focussed beamformer vs. inverse method," *Proceedings of the 10th International Congress on Sound and Vibration,* Stockholm, Sweden, 7-10 July, CD-ROM (2003).

[9] P.C. Hansen, "Analysis of discrete ill-posed problems by means of the L-curve," *SIAM Review* **34**, 561-580 (1992).

[10] P.C. Hansen and D.P. O'Leary, "The use of the L-curve in the regularization of discrete ill-posed problems," *SIAM Journal on Scientific Computing* **14**, 1487-1503 (1993).

APPENDIX

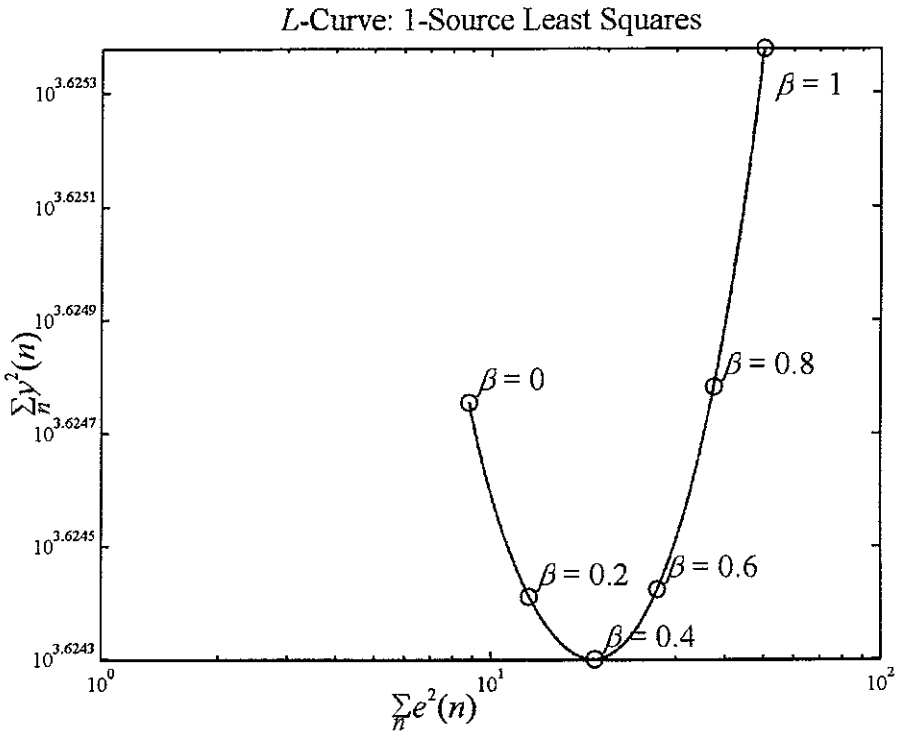

Figure A 1 - *L*-curve for 1-source least squares estimation.

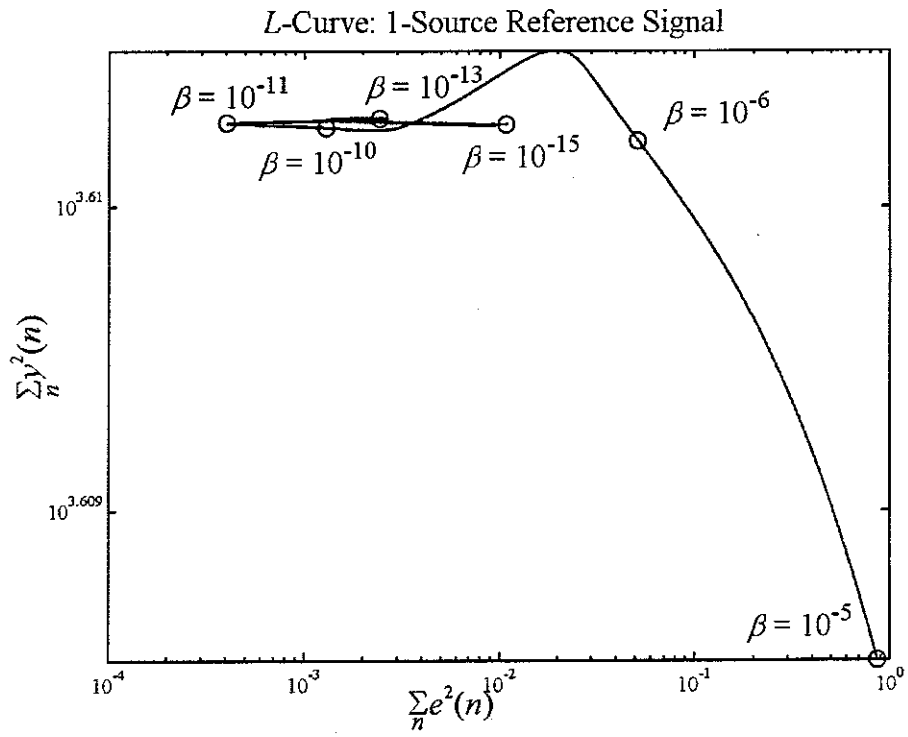

Figure A 2 - *L*-curve for 1-source reference signal method.

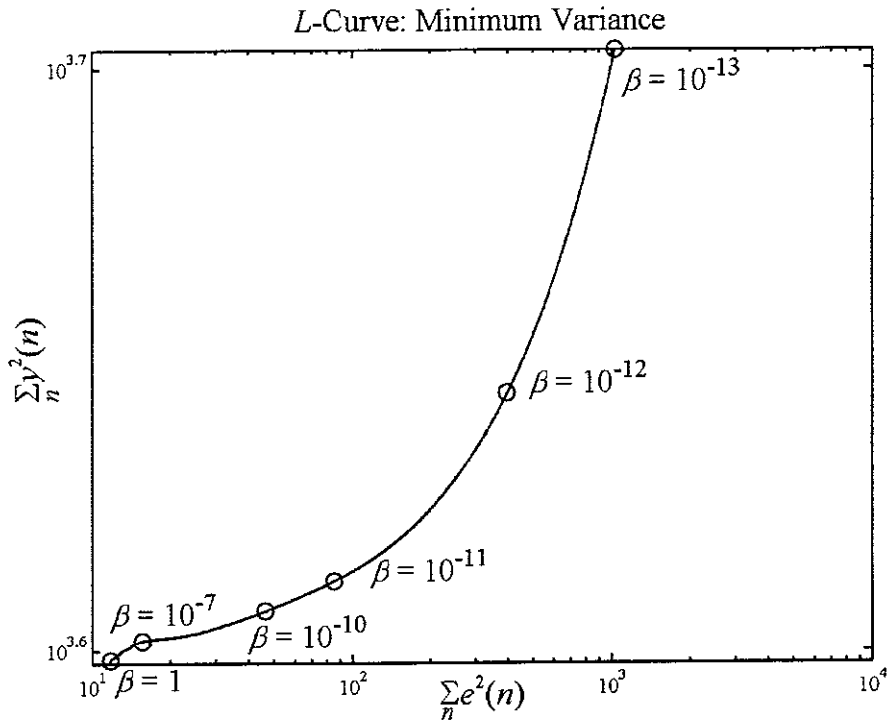

Figure A 3 - *L*-curve for minimum variance method.

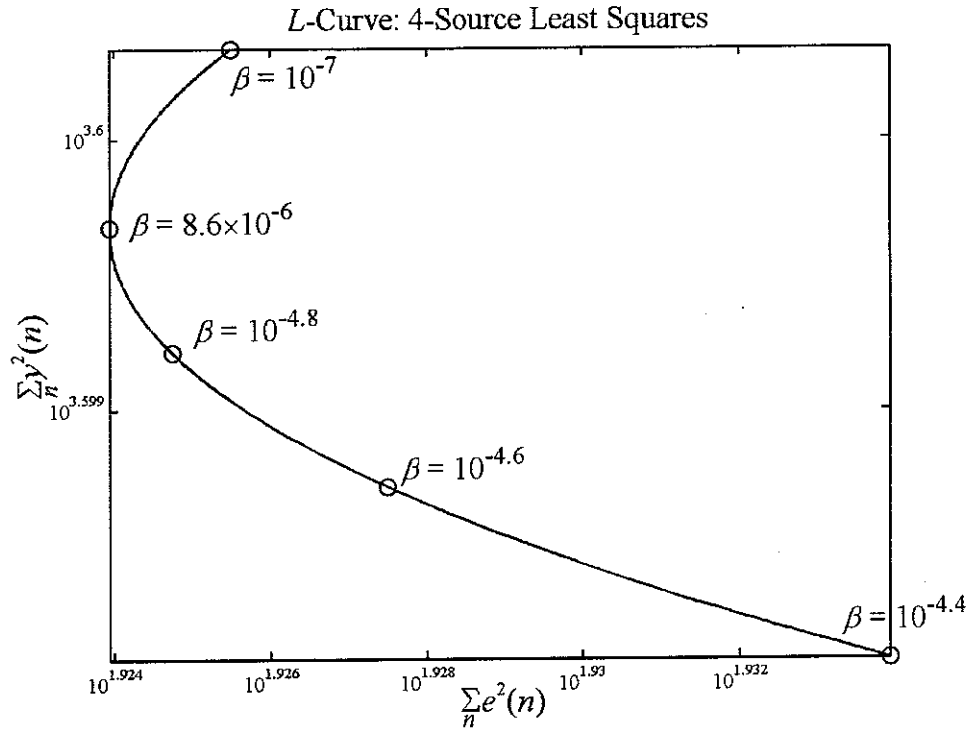

Figure A 4 - *L*-curve for 4-source least squares estimation.

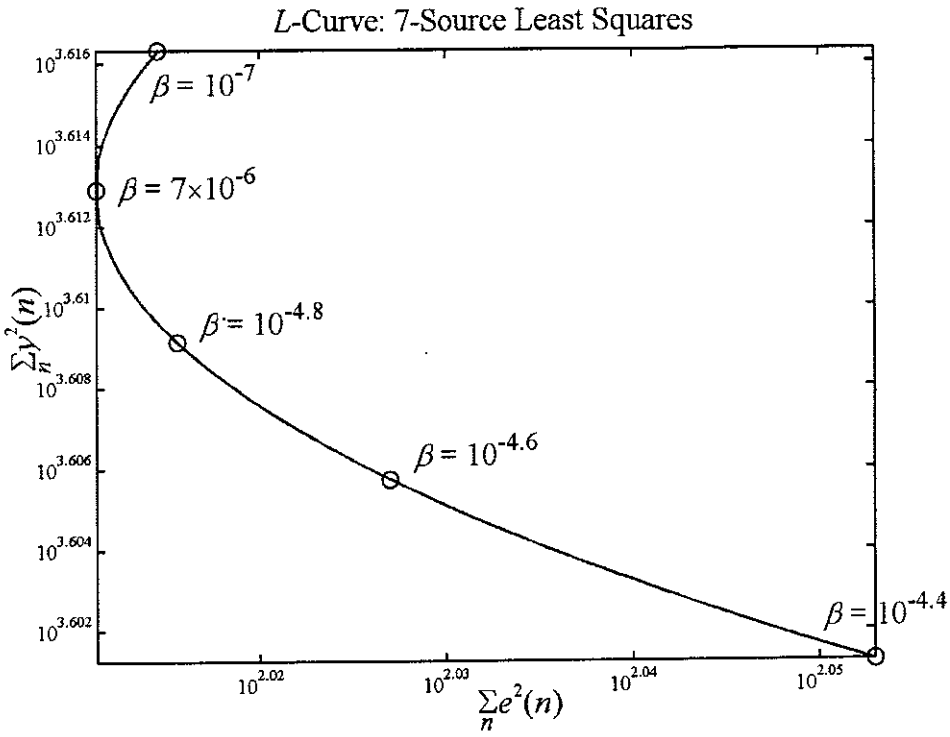

Figure A 5 - *L*-curve for 7-source least squares estimation.

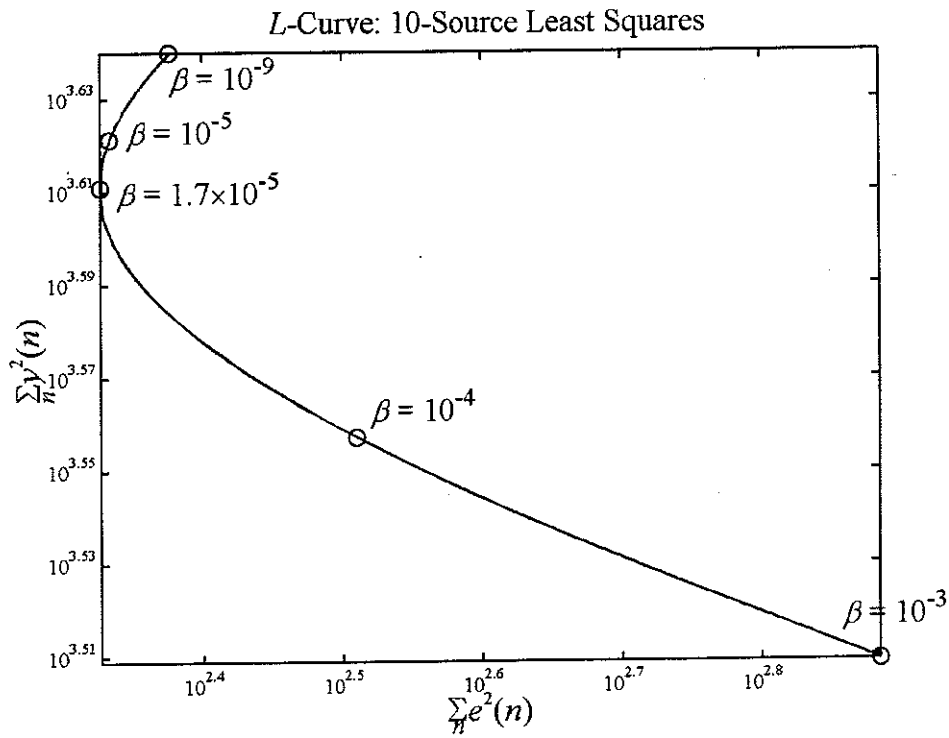

Figure A 6 - *L*-curve for 10-source least squares estimation.

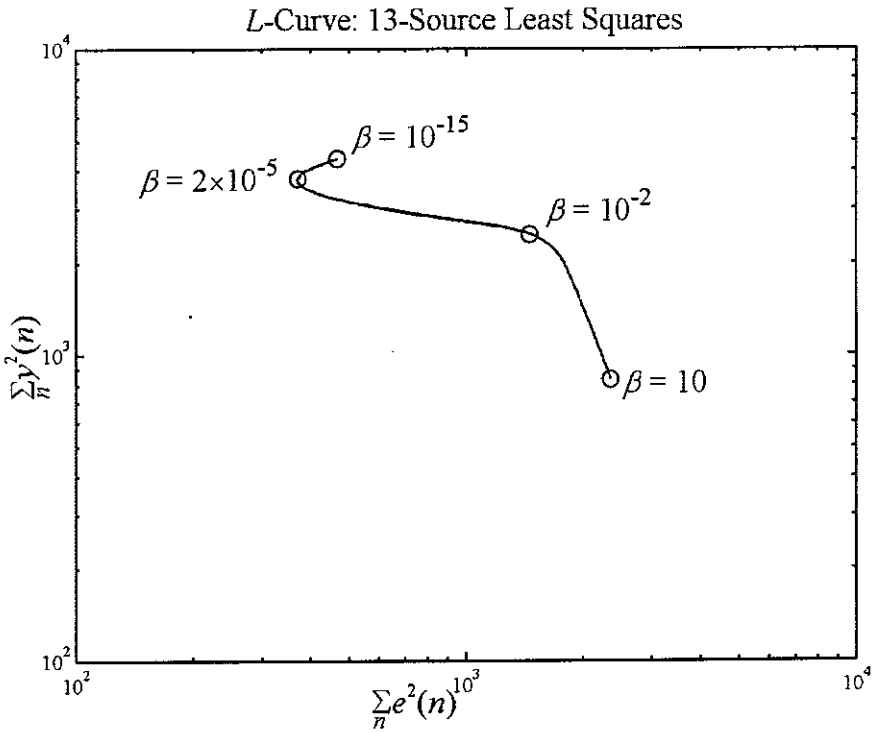

Figure A 7 - *L*-curve for 13-source least squares estimation.

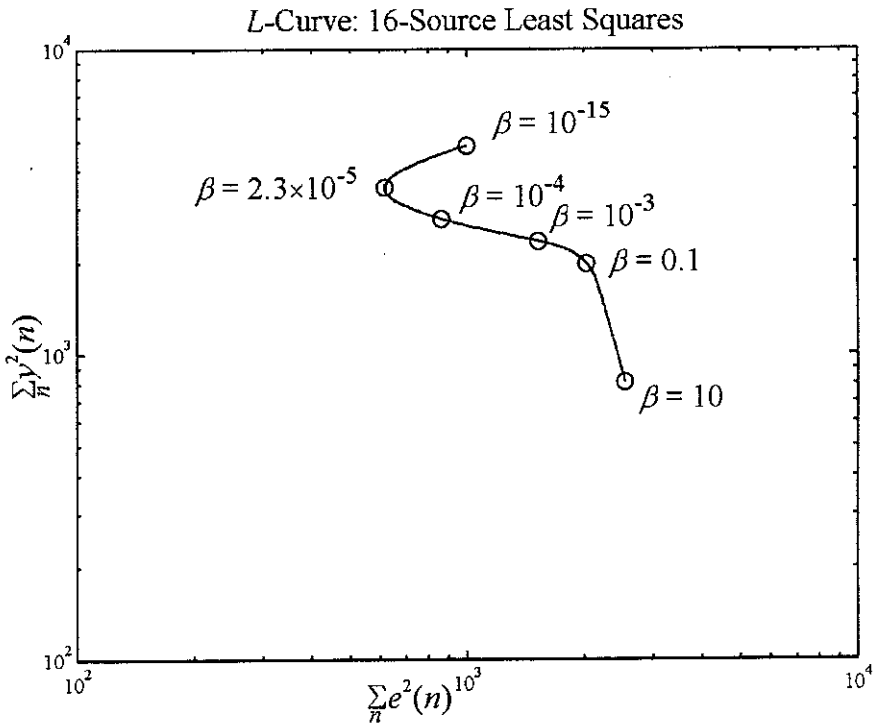

Figure A 8 - *L*-curve for 16-source least squares estimation.

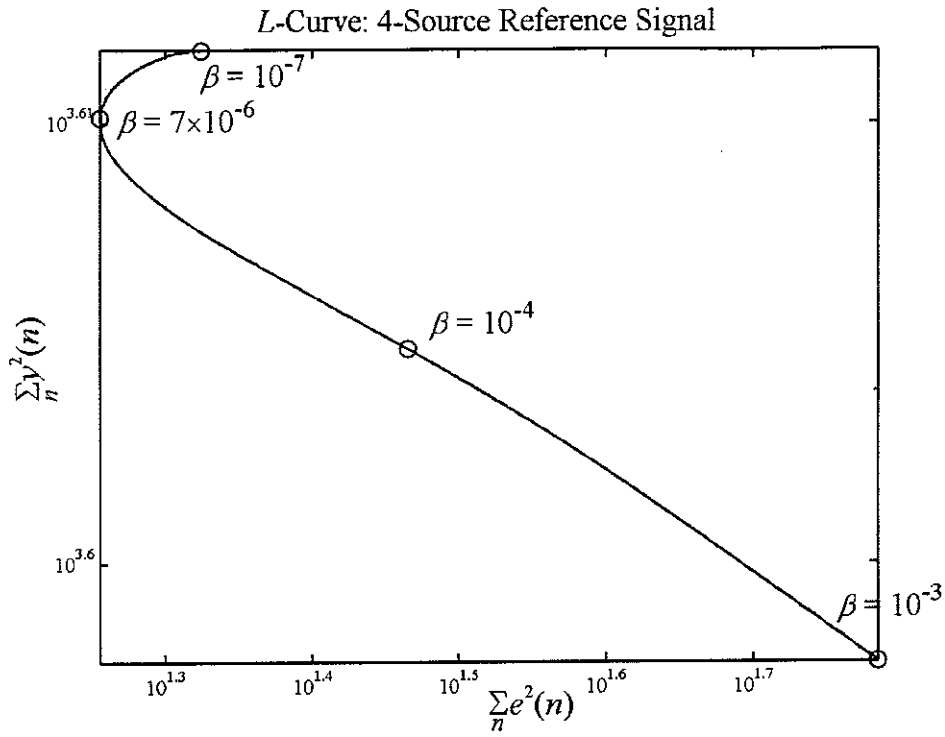

Figure A 9 - *L*-curve for 4-source reference signal method.

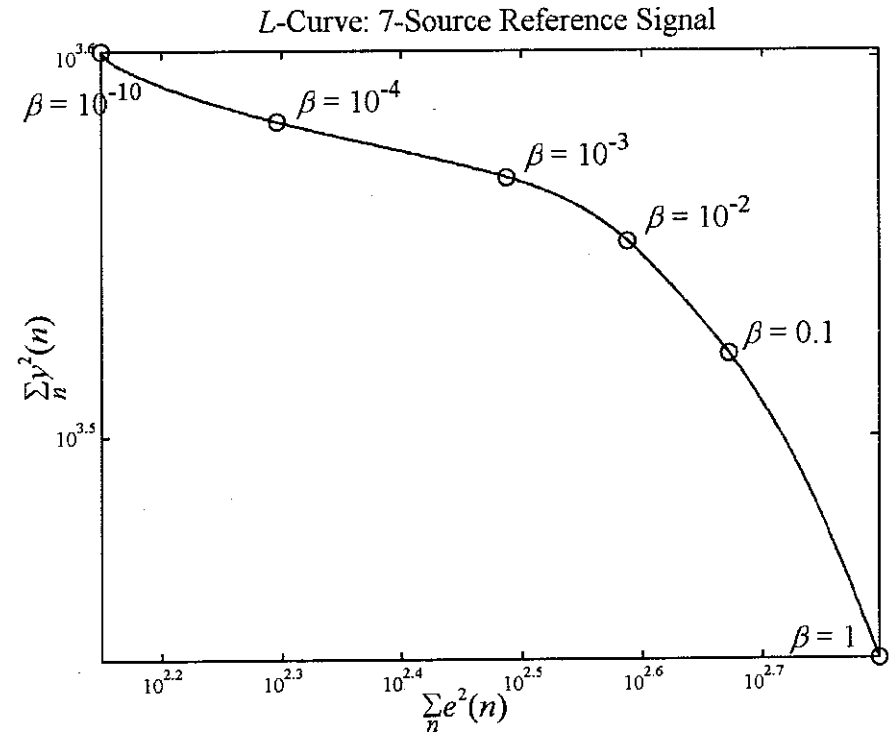

Figure A 10 - *L*-curve for 7-source reference signal method.

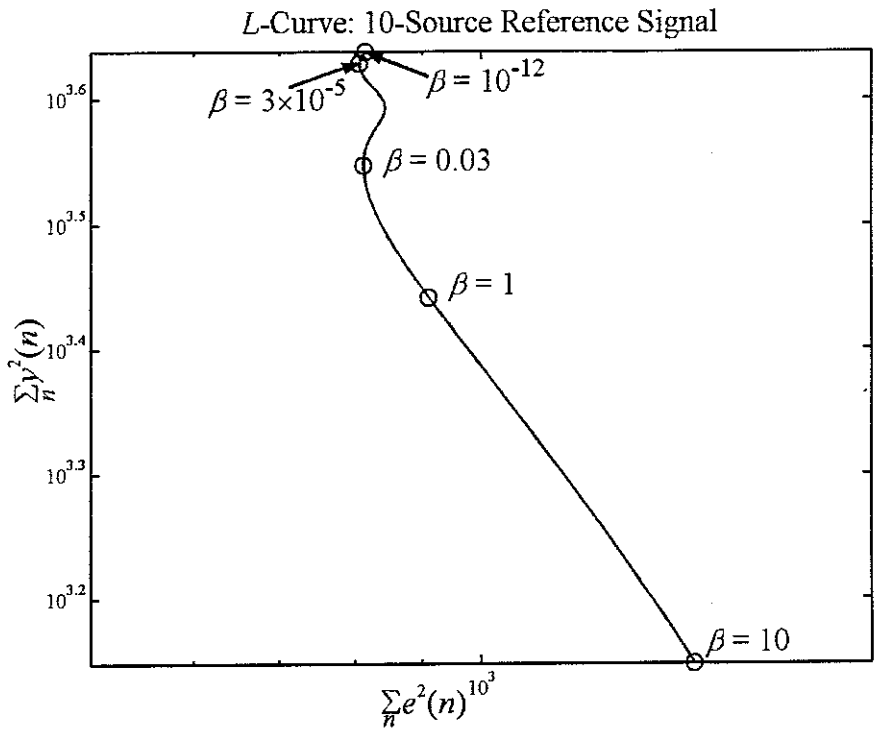

Figure A 11 - *L*-curve for 10-source reference signal method.

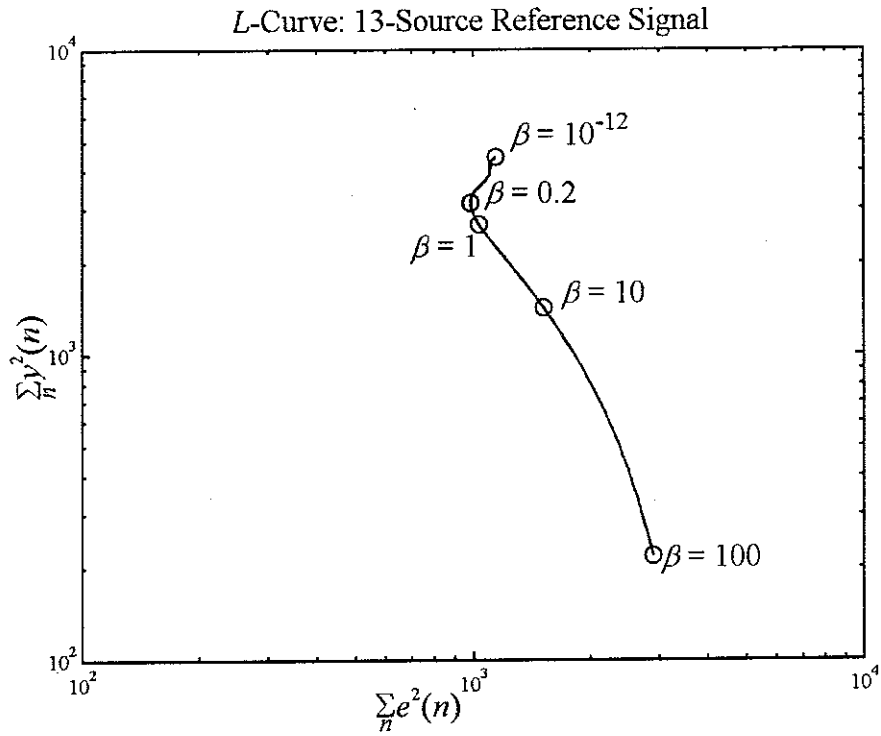

Figure A 12 - *L*-curve for 13-source reference signal method.

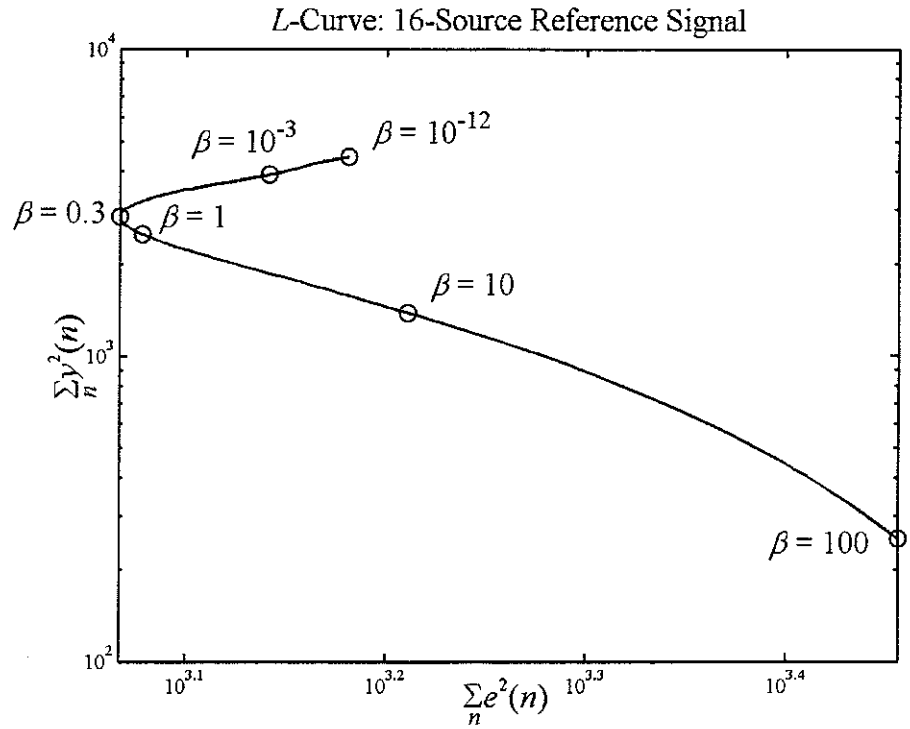

Figure A 13 - *L*-curve for 13-source reference signal method.